View metadata, citation and similar papers at core.ac.uk
brought to you by CORE
provided by KITopen

Simon Hammerich*
Marco Gleiß
Michael Kespe
Hermann Nirschl

An Efficient Numerical Approach for Transient Simulation of Multiphase Flow Behavior in Centrifuges

Solid bowl centrifuges are applied for the separation of small particles in a variety of industries. However, the particles accumulate at the rotor wall, which leads to a time-dependent separation efficiency. A numerical approach for spatial and time-resolved simulations of the separation process in a tube centrifuge is developed and some numerical results are presented. The back coupling of the dispersed and sedimented particles is realized by locally defined viscosity functions. The open source computation software OpenFOAM was used to simulate the turbulent multiphase flow within the centrifuge. The numerical investigations demonstrate the significant influence of the growing sediment on the flow conditions and of the rheological behavior of the sediment on the sediment shape.

Keywords: Centrifuges, Flow conditions, Rheological behavior, Sediments, Transient simulation

1 Introduction

In a variety of industries, the separation of dispersed solid par ticles from a continuous liquid phase is required, e.g., pharma ceutical, chemical, waste water treatment, and food industry [1, 2]. Centrifugal separation is often preferred to separate small particles due to the high achievable centrifugal forces and is used for a long time in industry. Nevertheless, only a simpli fied analytical approach, the so called sigma theory, is available for dimensioning centrifuges [3]. According to this theory, the spatial flow and sediment buildup are neglected. But especially in semicontinuous centrifuges, the particles accumulate at the rotor wall, i.e., they build a sediment which influences spatially and temporarily the flow conditions within the centrifuge, thus, leading to a time dependent separation efficiency.

The shape of the sediment determines the impact of the sedi ment on the flow conditions. However, the rheological behav ior of the sediment also influences strongly the sediment shape [4, 5]. Neglecting the sediment buildup, the theoretically pre dicted separation efficiency deviates significantly from the experimentally measured efficiency. As a result, costly experi ments in terms of raw materials and time are currently indis pensable to design centrifuges.

Due to growing computing power and developed simulation models, computational fluid dynamics (CFD) is an alternative to costly experiments. Full time and spatially resolved charac terizations of flow conditions are the key advantage. Self devel oped and standard approaches for the simulation of turbulent multiphase flows are known in literature [6]. While some researchers investigated the separation process in centrifuges with CFD [7 10], others took the influence of the sediment buildup into account [9, 11, 12]. Breitling et al. [7] observed that fully in time and spatially resolved simulations of the flow conditions are needed for the prediction of the separation pro cess in semi or continuous centrifuges. Gleiß et al. [13] devel oped a model for continuous centrifuges for flow sheet simula tions from CFD simulations.

A simulation approach is described, which is highly efficient in terms of required computational time compared to the resolved results, for considering the influence of the rheological behavior of the sediment on the sediment buildup. First, the general method is presented, followed by results of numerical investigations of the flow conditions in a tube centrifuge, depending on the sediment shape and the impact of the rheo logical behavior on the sediment buildup.

2 Method

2.1 General Approach

For spatial and temporal numerical simulations, an approach with a compromise between physical resolution and time con

Simon Hammerich, Marco Gleiß, Michael Kespe, Prof. Dr. Ing. Her mann Nirschl
Simon.Hammerich@kit.edu
Karlsruhe Institute for Technology (KIT), Institute for Mechanical Process Engineering and Mechanics, Straße am Forum 8, 76131 Karlsruhe, Germany.

sumptions equal to the fast Eulerian approach of Ferry and Balachander [14] was developed. The solid and liquid phases are approximated by a mixed phase. Solving the Navier Stokes equations for the mixed phase leads to the velocity field $\mathbf{v}_m(\mathbf{x},t)$[1)] where $\mathbf{x}$ is the spatial position and t is the time. With the information about the velocity field of the mixed phase, the movement of the dispersed phase can be evaluated explicitly by a transport equation. The dispersed phase is modeled as the local volume fraction of the particles. As a result, only one additional partial differential equation (PDE) has to be solved, leading to a lower time consumption compared to a classical Eulerian approach.

The presented approach is extended of the required reaction of flow conditions due to the growing sediment. This is realized by area defined viscosity functions depending on the local vol ume fraction of the particles. To take the complex rheological behavior into account, different viscosity functions are solved for the zone of the slurry and the sediment in the centrifuge. The method is implemented into the open source software OpenFOAM. So far, the gas phase is neglected. The approach is limited to the transport of an average particle size and can only treat incompressible sediments.

2.2 Transport of Particles

For the evaluation of the transport of the solid, an equation for the volume fraction α of the particle is solved. The PDE is giv en in Eq. (1):

$$\frac{\partial \alpha}{\partial t} + \mathbf{v}_p \nabla \alpha \quad \nabla\left(\frac{\eta_t}{S_t}\nabla\alpha\right) = 0 \tag{1}$$

η_t is the turbulent viscosity and S_t is the turbulent Schmidt number. The local velocity of the particle $\mathbf{v}_p$ is the summation of the mixed phase velocity $\mathbf{v}_m$ and the local sedimentation velocity $\mathbf{v}_s$ of the particle, which is given in Eq. (2).

$$\mathbf{v}_p(\mathbf{x},t) = \mathbf{v}_m(\mathbf{x},t) + \mathbf{v}_s(\mathbf{x},t) \tag{2}$$

The approach of Stokes et al. [15] is generally applied for the theoretical prediction of the sedimentation process, but it is only suitable for small particle Reynolds numbers, $Re_p < 0.25$. For the method, a more general approach for the calculation of the sedimentation velocity $\mathbf{v}_{ssp}$ of a single, spherical particle in the centrifugal field was chosen, which was evolved [16] from Stokes approach and is presented in Eq. (3).

$$\mathbf{v}_{ssp} = \left(\frac{4}{3}\frac{\rho_p}{\rho_l}\frac{d_p}{c_D(\mathrm{Re}_p)}\left(1 \quad \frac{\rho_p}{\rho_l}\right)\omega^2 r\right)^{\frac{1}{2}} \tag{3}$$

ρ_p is the density of the particle, ρ_l is the density of the liquid, d_p is the particle size, and c_D is the drag force coefficient, which is dependent of the Reynolds number Re_p of the particle; ω denotes the angular velocity and r is the radius. The drag force coefficient is calculated by the correlation of Kürten et al. [17], which is valid up to $Re_p < 2\times10^5$ and defined in Eq. (4).

$$c_D(Re_p) = \frac{21}{Re_p} + \frac{6}{\sqrt{Re_p}} + 0.28 \tag{4}$$

The sedimentation velocity presented in Eq. (2) is only valid for a single particle. To transfer this velocity onto a bulk of par ticles, the particle interference has to be taken into account. Therefore, Eq. (2) is adjusted by the approach of Michaelis and Bolger [18]. The corrected equation for the calculation of the sedimentation velocity is given in Eq. (5):

$$\mathbf{v}_s = \left(1 \quad \frac{\alpha}{\alpha_{gel}}\right)^{n_{hs}} \mathbf{v}_{ssp} \tag{5}$$

The sedimentation velocity is dependent on the volume frac tion of the particle at the gel point α_{gel} and the coefficient n_{hs}.

2.3 Packing Limiter

The volume fraction α is only valid in the range of $\alpha \varepsilon [0,1]$. Here, the solid phase exists as dispersed particles, the maxi mum level of α is much smaller as 1. The highest packing den sity of monodisperse and spherical particles is $\alpha \approx 0.74$, simul taneously the packing density is depending on the material behavior of the treated particles. To take this physical behavior into account, a packing limiter is implemented.

2.4 Rheological Behavior

The rheological behavior of the treated materials has a major influence on the separation process in the centrifuge. The dynamic viscosity η is the presenting parameter for the rheo logical behavior in computational fluid dynamics and is the ratio of the shear stress τ and the shear rate $\dot{\gamma}$, as shown in Eq. (6).

$$\eta = \frac{\tau}{\dot{\gamma}} \tag{6}$$

The material behavior changes totally at the crossover from suspension to sediment due to the particle particle contacts in the framework. Owing to this physical behavior, two different viscosity functions are used for modeling the different rheologi cal behavior.

2.4.1 Suspension

For modeling the influence of the volume fraction of the parti cle on the dynamic viscosity of the suspension η_{susp}, the approach of Quemada [19], which is given in Eq. (7), is applied, in which η_l is the dynamic viscosity of the pure liquid. Effects like shear thinning or shear thickening and a possible emerg ing yield point are neglected.

1) List of symbols at the end of the paper.

$$\eta_{\text{susp}} = \eta_{\text{l}} \frac{1}{\left(1 \quad \frac{\alpha}{\alpha_{\text{gel}}}\right)^2} \tag{7}$$

2.4.2 Sediment

The rheological behavior of a saturated sediment plays an essential role in the sediment buildup. Saturated sediments show complex rheological behavior due to viscous friction in the pore fluid and coulomb friction at particle particle contact [20, 21] resulting in a compressive yield stress p_{s} depending yield locus [22]. Erk [20] and Mladenchev [21] investigated the influence of various parameters on the rheological behavior of saturated sediments. Both authors propose an approach, which is presented in Eq. (8), similar to a Herschel Bulkley fluid to model the flow properties.

$$\tau_{\text{sed}}(p_{\text{s}}) = \tau_0(p_{\text{s}}) + K(p_{\text{s}})\dot{\gamma}^{n_{\text{rheo}}(p_{\text{s}})} \tag{8}$$

where τ_{sed} is the shear stress in the sediment, τ_0 is the yield point, K is the consistency, and n_{rheo} denotes the rheological coefficient. Each parameter can be dependent on the local com pressive yield stress. The sediment shape is influenced by the flow properties.

In Fig. 1, two extreme cases of shapes due to different rheo logical behavior are presented. A sediment with a high yield point forms a shape with a high slope, and with a very low yield point it will spread uniformly in the rotor due to particle move ment. The movement of the sediment derives from the super position of flowing and gliding. As gliding cannot be repro duced with this simplified method, both processes are merged together and modeled as a virtual viscosity of the sediment η_{sed}.

As discussed, the two viscosity functions for suspension and sediment have to be handled together for the mixed phase. This is realized by the summation and weighting of both functions with the suspension coefficient A and sediment coefficient B, as defined in Eq. (9). An algorithm to recognize the area of the suspension and sediment is implemented to set the value of A and B. In the area of the suspension, A is set to 1 and B to 0, for the sediment inversely. The viscosity of a sediment is infin ity as long it is not flowing. Given that infinity cannot be handled by a computer, the viscosity of the sediment has to be leveled.

$$\eta_{\text{m}} = A\eta_{\text{susp}} + B\eta_{\text{sed}} \tag{9}$$

2.5 Algorithm

The method is optimized to minimize the required computing time for the simulations. The transient separation process is modeled as a quasi station ary process. It is assumed that the influence of the particles on the flow conditions for a short period of time can be neglected. Therefore, for the short period of time only the solid transport is calculated. After this period, the Navier Stokes equations are solved until reaching stationary flow con ditions.

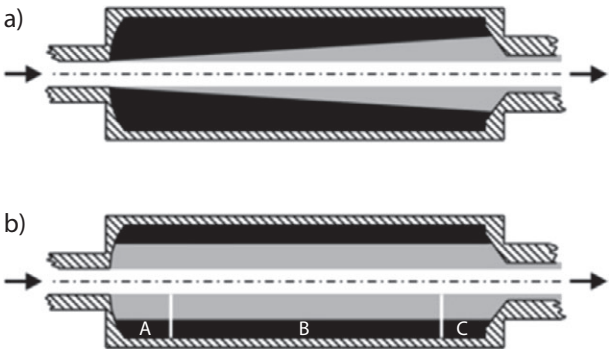

Figure 1. Variation of the sediment buildup depending on the rheological behavior in a tubular centrifuge: (a) high-yield point, (b) low-yield point [4]. A,B, and C are zones with different expected flow conditions within the centrifuge: (A) turbulent inlet zone, (B) zone of nearly constant flow conditions, (C) outlet zone.

The algorithm of the method is schematically presented in Fig. 2. Two extra variables are needed; t_{crit} is the length of the short period in which only the particle transport is solved and t_{help} is a time counter. With this handling, it is possible to reduce the computing time up to 98 % with an acceptable nega tive effect on the simulation results.

3 Geometry and Parameter

For testing the described method, simulations with a simplified geometry of a rotor of a tube centrifuge were performed. The geometry with the used mesh is presented in Fig. 3. In the middle of the rotor is a solid core to repress the gas core. Hence, the gas phase can be neglected and only the liquid and solid phases have to be taken into account. The suspension flows fully accelerated into the geometry at the inlet patches. The mesh is totally struc tured with a grading towards the walls of the rotor.

For modeling the turbulence, the kOmegaSST turbulence model is applied. The laminar boundary layer is fully resolved, hence, no special wall function for turbulence modeling is required. The rotor has a length of 0.167 m, an outer diameter

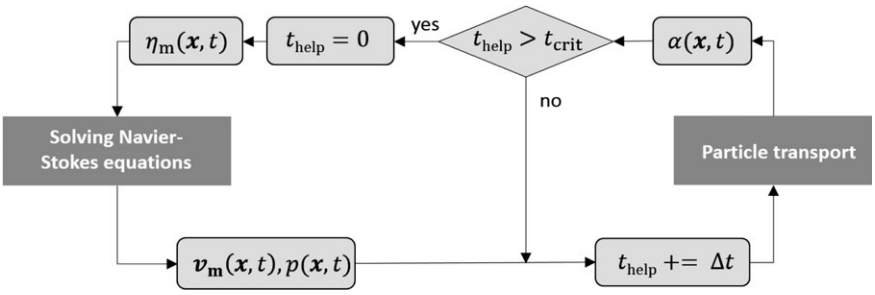

Figure 2. Schematic algorithm for the quasi-stationary modeled separation process in centrifuges; t_{help} is a time counter and t_{crit} is the length of the interval in which only the particle transport is calculated.

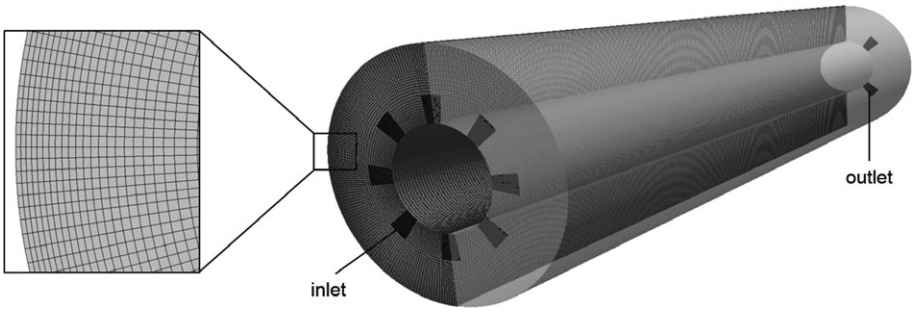

Figure 3. Simplified geometry of a rotor of a tube centrifuge and the used mesh. A mesh grading towards the walls is realized.

of 0.038 m, and an inner diameter of 0.016 m. At the beginning of the simulations, the rotor is filled with pure liquid and the flow conditions are fully evolved. The presented sediments are incompressible and the consolidation zone of the sediment is reduced to the size of one cell. The chosen process parameters and material properties, except the rheological behavior, are given in Tab. 1.

Table 1. Chosen material properties, except the rheological behavior, and process parameters used for the presented numerical simulations.

Parameter	Value
Material properties	
Fluid density ρ_l [kg m ^{3}]	1000
Particle density ρ_s [kg m ^{3}]	2500
Dynamic viscosity of the pure fluid η_l [kg m ^{1}s ^{1}]	1.0×10^{3}
Particle diameter d_p [m]	30×10^{6}
Porosity of the sediment ε [ ]	0.5
Process parameters	
Volume fraction of the particles at the inlet α [ ]	0.02
Volumetric flow rate $\dot{V}$ [m^{3}s ^{1}]	8.33×10^{6}
Angular velocity ω [s ^{1}]	200

4 Results

4.1 Sediment Buildup and Influence on the Flow Conditions

The flow conditions inside the rotor determine the separation efficiency. During the separation process, a sediment arises and changes in time. The sediment is an area of a porous media. Due to the higher pressure loss for the fluid in the sediment, the sediment influences critically the flow conditions within a centrifuge. Changes of the sediment during the process lead to a time dependent separation efficiency. Hence, it is crucial for the simulation method to reproduce this behavior.

The method models the sediment by an area of different rheological behavior as the suspension or pure fluid. This leads to a different energy drop in the sediment as in the suspension. The energy drop in the sediment reproduces quite the same effect on the flow conditions as the pressure loss of a porous media. Only a possible marginal flow through the sediment has to be neglected. Fig. 4 illustrates the influence of the sediment on the flow conditions. Therefore, only the axial velocity $\mathbf{v}_{ax}$ and the solid fraction α are presented for different simulation times t_{sim} near the inlet.

In Figs. 4 a and b, the sediment is shown for 0 and 50 s simulation time. At 0 s simulation time no sediment is formed. In Figs. 4 c and d, the axial velocity is presented for the different times. The axial flow is totally dependent on the inlet and outlet geometry. Here, a fast axial flow near the inner wall with a zone of slow vortexes towards the outer wall occurs in the machine. This observation is conform to the boundary layer theory [2]. At 50 s simulation time, a sediment has arisen next to the inlet, which is presented as the local volume fraction of the particles. The influence of the sediment onto the flow conditions is obvious. In the area of the sediment no axial flow exists and where the sediment rises into the boundary layer, the axial velocity increases due to a reduction in space.

Quantitative changes of the axial velocity due to the sediment are indicated in Fig. 5. The sediment height (Fig. 5 a) and the axial velocity at two positons (Figs. 5 b and c) are presented for 0, 50, 100, and 200 s process time. The inflow of particles start at a process time of 0 s, therefore, the sediment height at 0 s is not shown. The position of the inlet coincides with the axial position $\mathbf{x}_{ax}$ of 0 m.

The particles settle down in the first few centimeters of the centrifuge. This leads to an unequally distributed sediment. With time, the sediment grows in height and towards the outlet, but a small passage between sediment and inner wall is kept clear. The reason for this is the increase of the axial velocity due to the growing sediment. The influence of the sediment on the flow conditions is illustrated in Figs. 5 b and c. Therefore, the axial velocities according to the radius for two different axial positions are presented in position 1 at 0.01 m and position 2 at 0.08 m. A boundary layer of a fast axial flow is recognizable near the inner wall. At position 1, axial vortices occur towards the outer wall by comparison to position 2.

With increasing sediment height at position 1, the flow conditions change dramatically. The higher energy loss due to the higher viscosity leads to an elimination of an axial flow in the area of the sediment, at the same time the axial flow increases near the inner wall. The acceleration of the axial flow converges to a limit due to the maximum sediment height. Although the sediment has not reached position 2, the flow conditions change. Due to the increase of the axial velocity near the inlet, vortices occur in the middle of the centrifuge leading to a higher local dispersion during the separation process. This proofs that a local sediment influences the global flow conditions in the machine.

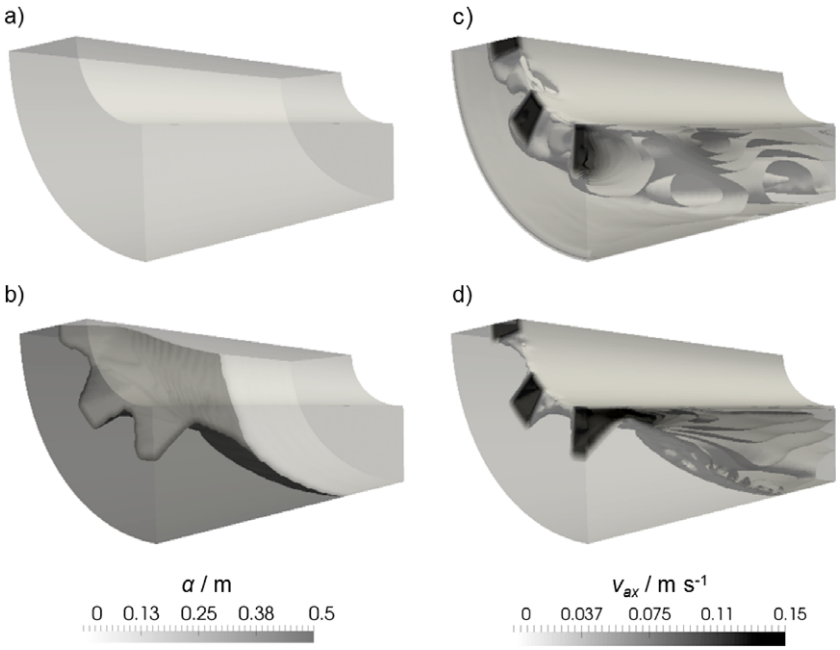

Figure 4. Influence of the sediment on the axial velocity. Sediment (a) at 0 s and (b) after 50 s simulation time. Axial velocity for (c) 0 s and (d) 50 s simulation time. The simulations start with fully evolved flow conditions within the centrifuge.

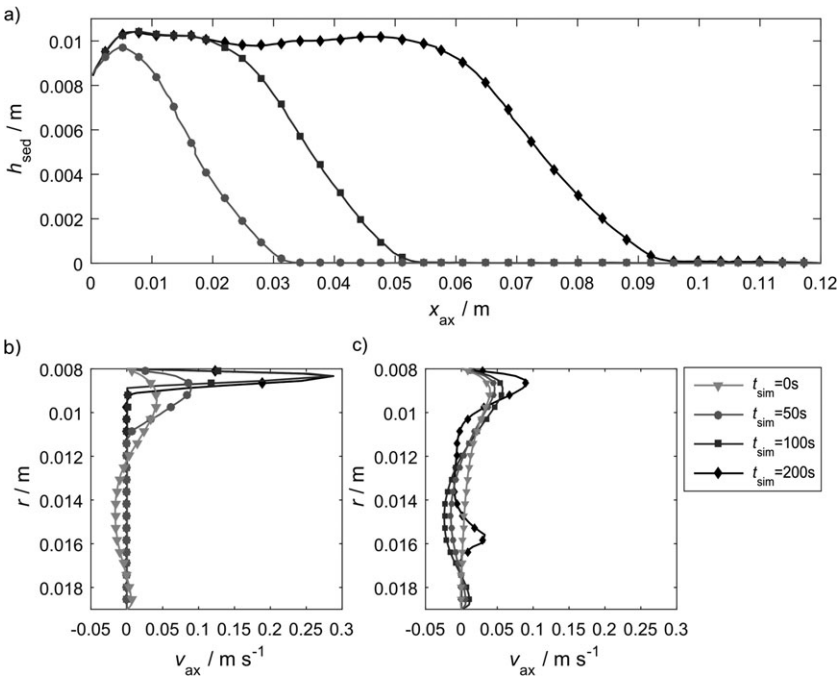

Figure 5. (a) Emerging sediment. At 0 s simulation time the separation process has not started, so no sediment is observed. (b) Axial velocity depending on the radial position at position 1 and (c) at position 2. Position 1 is at the axial position of 0.01 m and position 2 at 0.08 m.

4.2 Influence of the Rheological Behavior of the Sediment

Not only the sediment has a crucial impact on the flow conditions, but also the flow conditions influence the sediment shape depending on its rheological behavior. In Fig. 6, simulations of a poor flowing (Fig. 6 a) and an easy flowing (Fig. 6 b) sed iment are presented. The axial flow is from left to right in the centrifuge. Every param eter is kept constant in both simulations, except the rheological behavior. The simu lation method responds as expected and a dramatic change of the sediment shape is observed. The poor flowing sediment emerges close to the area of the inlet and evolves a steep slope. Compared to this, the easy flowing sediment spreads more equally along the outer wall, where it changes to a more even slope.

To investigate the impact of the rheologi cal on the sediment shape, an empiric nu merical study with variation of material properties of the sediment was performed. A simplified viscosity function to model the behavior was used, in which only the yield point is a function of the compressive yield stress and every parameter is kept constant during the simulations. A linear influence of the compressive yield stress was chosen. The used function for calculat ing the local yield point is defined in Eq. (10) where y is the yield point at $p_s = 0$ and q is the proportionality factor.

$$\tau_0(p_s) = qp_s + y \tag{10}$$

The parameters for the rheological be havior of four exemplarily chosen simula tions are presented in Tab. 2. The value of each parameter was selected in considera tion of the process parameters of the simu lated separation processes.

Fig. 7 displays the average sediment height after 60 s process time of the four selected simulations. All kinds of different slopes and inhomogeneity disposition are observed. From behavior 1 to 4, the flow ability of the sediment increases. With higher flowability, the slope of the sediment decreases and the sediment spreads more even along the rotor. Hence, the sediment shape is totally dependent on the rheologi cal behavior. With the empiric study it was identified that each parameter of the chosen viscosity function can be crucial for the sediment shape. Due to the fact that the sediment shape has a fundamental impact on the flow condi tions, accurate knowledge of the rheological behavior is essen

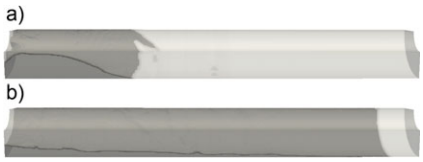

Figure 6. Comparison of the sediment buildup of (a) a poor-flowing and (b) an easy-flowing sediment after a simulation time of 50 s. Process and material parameters are kept constant, except the flow behavior.

Table 2. Parameters for describing the rheological behavior of the sediment of four exemplary simulations, presented in Fig. 7.

	q [ ]	y [Pa]	K [Pa s]	n [ ]
Rheological behavior 1	2.5	5000	1×10^{4}	1
Rheological behavior 2	0.5	500	1×10^{6}	1
Rheological behavior 3	0.001	30	1×10^{3}	1
Rheological behavior 4	0.001	30	1×10^{4}	1

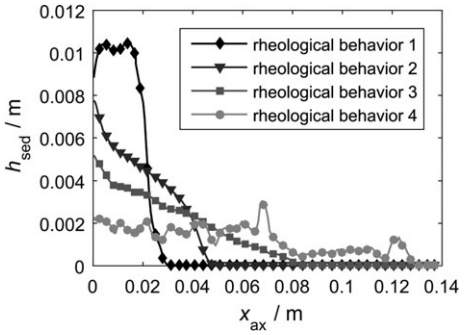

Figure 7. Sediment shape after 60 s simulation time of four different rheological behaviors. Changes of the rheological behavior lead to obvious alterations in the sediment shape.

tial for a valuable numerical prediction of the separation process. However, the main outcome is that the developed approach is suitable for the simulation of the separation process considering the sediment buildup with different rheological behavior.

5 Conclusions

An efficient method for computational fluid dynamic simulations of separation processes in centrifuges was developed. The multiphase flow within a centrifuge is reduced to a mixed phase. Besides the Navier Stokes equations for the mixed phase, the particle transport is explicitly calculated by a transport equation. The back coupling of the particles onto the flow conditions is performed by the rheological behavior of the mixed phase. The approach allows the handling of a wide range of different rheological behaviors of sediment and suspension.

The presented simulation method allows spatially and temporally resolved simulations in due consideration the sediment buildup and flowing in solid bowl centrifuges. The numerical investigations showed that the sediment has a crucial impact on the flow conditions, thus onto the separation efficiency. Even a locally limited sediment affects the flow conditions within the whole machine. The performed simulations demonstrated that the rheological behavior of the sediment influences dramatically the shape of the sediment. Therefore, the knowledge of the rheological behavior of the sediment is crucial for an accurate prediction of the separation efficiency of a centrifuge with numerical simulations.

Acknowledgment

The authors would like to thank the German research association "Allianz Industrie und Forschung" for funding this project (IGF 18461 N).

The authors have declared no conflict of interest.

Symbols used

A	[ ]	suspension coefficient
B	[ ]	sediment coefficient
c_D	[ ]	drag coefficient
d	[m]	diameter
K	[Pa s^n]	consistency
n	[ ]	coefficient
p_s	[Pa]	compressive yield stress
q	[ ]	proportionality factor
r	[m]	radius
Re	[ ]	Reynolds number
S	[ ]	Schmidt number
t	[s]	time
$\mathbf{v}$	[m s^{-1}]	velocity
$\dot{V}$	[$m^3 s^{-1}$]	volumetric flowrate
$\mathbf{x}$	[m]	spatial position
y	[Pa]	yield point at zero compressive yield stress

Greek letters

α	[ ]	particle volume fraction
$\dot{\gamma}$	[s^{-1}]	shear rate
ε	[ ]	porosity
η	[Pa s]	dynamic viscosity
ρ	[kg m^{-3}]	density
τ	[Pa]	shear stress
τ_0	[Pa]	yield point
ω	[s^{-1}]	angular velocity

Subscripts

ax	axial
crit	critical
gel	gel point
help	counter
hs	hindered settling
l	liquid
m	mixed phase

p	particle
rheo	rheological
s	sedimentation
sed	sediment
sim	simulation
ssp	single, spherical particle
susp	suspension
t	turbulent

Abbreviations

CFD	computational fluid dynamics
PDE	partial differential equation

References

[1] H. Anlauf, *F&S, Filtr. Sep.* **2012**, *26 (3)*, 230 238.
[2] W. Leung, *Industrial Centrifugation Technology*, McGraw Hill, New York **1998**.
[3] C. M. Ambler, *J. Biochem. Microbiol. Technol. Eng.* **1959**, *1 (2)*, 185 205.
[4] S. Stahl, L. E. Spelter, H. Nirschl, *Chem. Eng. Technol.* **2008**, *31 (11)*, 1577 1583.
[5] L. E. Spelter, H. Nirschl, A. D. Stickland, P. J. Scales, *AIChE J.* **2013**, *59 (10)*, 3843 3855.
[6] A. Paschedag, *CFD in der Verfahrenstechnik*, Wiley VCH, Weinheim **2004**.
[7] M. Breitling, U. Janoske, M. Piesche, *Chem. Ing. Tech.* **2003**, *75 (3)*, 184 188.
[8] R. Burger, F. Concha, *Int. J. Miner. Process.* **2001**, *63*, 115 145.
[9] C. Pang, W. Tan, E. Sha, Y. Tao, L. Liu, *Front. Chem. Sci. Eng.* **2012**, *6 (3)*, 329 338.
[10] X. Romani Fernandez, *Ph.D. Thesis*, Karlsruhe Institute of Technology, **2012**.
[11] R. Burger, M. C. Bustos, F. Concha, *Int. J. Miner. Process.* **1999**, *55*, 267 282.
[12] M. Gleiss, H. Nirschl, *Chem. Eng. Technol.* **2015**, *38 (10)*, 1873 1882.
[13] M. Gleiss, S. Hammerich, M. Kespe, H. Nirschl, *Chem. Eng. Sci.* **2017**, *163*, 167 178.
[14] J. Ferry, S. Balachandar, *Int. J. Multiphase Flow* **2001**, *27 (7)*, 1199 1226.
[15] S. G. G. Stokes et al., *Mathematical and Physical Papers*, University Press, Cambridge **1901**.
[16] M. Beiser, *Dissertation*, University Karlsruhe (TH), **2006**.
[17] H. Kurten, J. Raasch, H. Rumpf, *Chem. Ing. Tech.* **1966**, *38 (9)*, 941 948.
[18] G. H. Meeten, *Colloids Surf., A* **1994**, *82 (1)*, 77 83.
[19] D. Quemada, *Rheol. Acta* **1977**, *16 (1)*, 82 94.
[20] A. Erk, *Ph.D. Thesis*, University Karlsruhe (TH), **2006**.
[21] T. Mladenchev, *Ph.D. Thesis*, University Magdeburg, **2007**.
[22] A. W. Jenike, *Storage and Flow of Solids*, Bulletin of the Uni versity of Utah No. 123, 7th rev. ed., University of Utah, Salt Lake City **1970**, 10 16.

Karlsruher Institut für Technologie

OPEN ACCESS

Repository KITopen

Dies ist ein Postprint/begutachtetes Manuskript.

Empfohlene Zitierung:

Hammerich, S.; Gleiß, M.; Kespe, M.; Nirschl, H.
An Efficient Numerical Approach for Transient Simulation of Multiphase Flow Behavior in Centrifuges.
2018. Chemical engineering & technology, 41.
doi: 10.5445/IR/1000084288

Zitierung der Originalveröffentlichung:

Hammerich, S.; Gleiß, M.; Kespe, M.; Nirschl, H.
An Efficient Numerical Approach for Transient Simulation of Multiphase Flow Behavior in Centrifuges.
2018. Chemical engineering & technology, 41 (1), 44–50.
doi:10.1002/ceat.201700104

Lizenzinformationen: KITopen-Lizenz